Supporting Information

Highly Efficient and Recyclable Chiral Phosphine-Functionalized Polyether Ionic Liquids for Asymmetric Hydrogenation of β-keto esters

Fan Wang [a, b], Shuai Zhang [b], Congxia Xie [a], Xin Jin [b, *]

[a] College of Chemistry and Molecular Engineering, Qingdao University of Science and Technology, 53 Zhengzhou Road, Qingdao 266042, China

[b] College of Chemical Engineering, Qingdao University of Science and Technology, 53 Zhengzhou Road, Qingdao 266042, China

Corresponding author e-mail: jinx1971@163.com.

Table of Contents

1. Calculation method for TON and TTON in Fig. 4

$$TON = \frac{n(MAA)}{n(catalyst)} \times Yield \quad (1)$$

$$TTON = \sum_{m=1}^{12} TON_m \quad (2)$$

m represents the runing numbers of the catalyst.

2.The air stability of Ru-3a catalyst

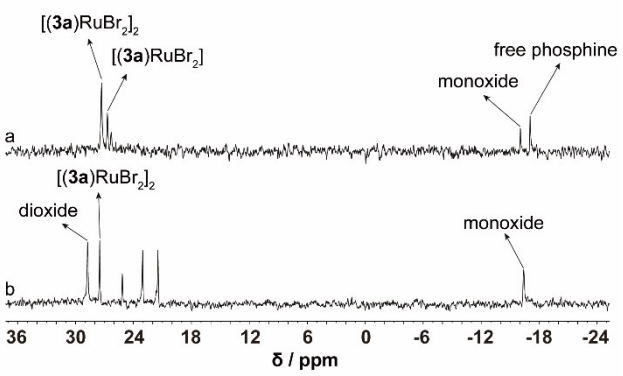

Fig. S1 ^{31}P NMR spectra of Ru-**3a** catalyst (202 MHz, DMSO-d_6). (a) fresh catalyst; (b) air stability testing, condition: 2 mL MeOH, T = 60 °C, t = 20 h, 4.6 MPa nitrogen atmosphere with 0.5% oxygen.

3. The thermal stability of Ru-3a catalyst

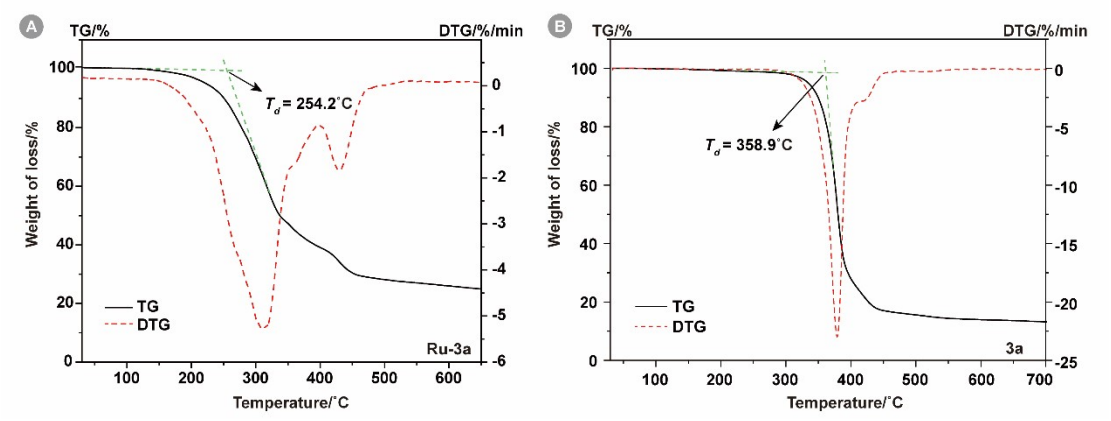

Fig. S2 TG profiles of Ru-**3a** catalyst (A) and **3a** (B).

4. The moisture stability of Ru-3a catalyst

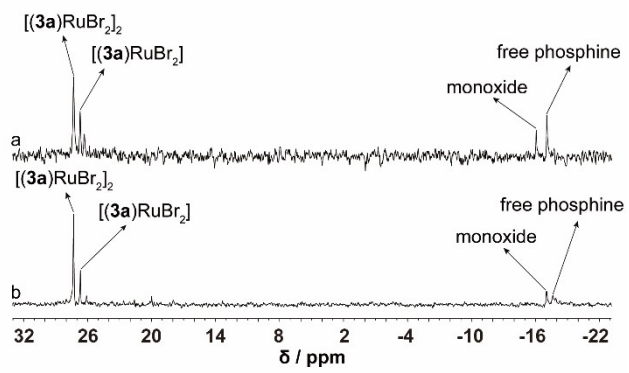

Fig. S3 ^{31}P NMR spectra of Ru-**3a** catalyst (202 MHz, DMSO-d_6). (a) fresh catalyst; (b) moisture stability testing, condition: 2mL methanol solution containing 3wt% water, T = 60°C, t = 20 h, $P(H_2)$ = 4.6 MPa.

5. Comparison of our work with previous reports for asymmetric hydrogenation of β-keto esters

Table S1 Comparison of our work with previous reports for asymmetric hydrogenation of β-keto esters

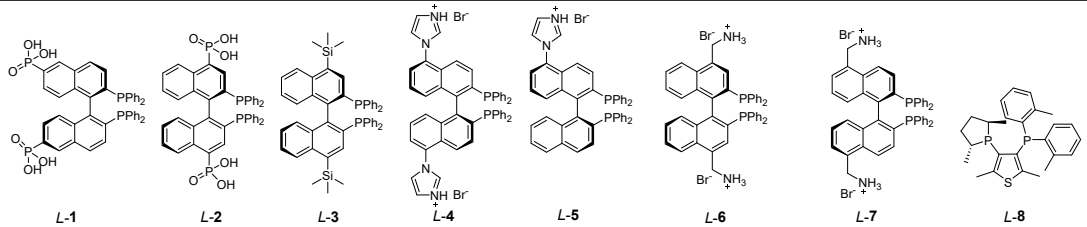

L-**1** *L*-**2** *L*-**3** *L*-**4** *L*-**5** *L*-**6** *L*-**7** *L*-**8**

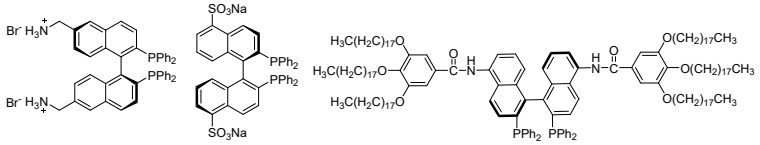

L-**9** *L*-**10** *L*-**11**

Entry	System	Reaction Medim	Ligand	Carrier IL/S [a] (mol%)	TOF [b] (h^{-1})	ee	TTON	Ru Loss (%)	Ref.
1 [c]	IL-homogeneous	[BMIm][BF_4]/MeOH	*L*-**1**	580	4.5	98.3	440	0.02	1
2 [c]	IL-homogeneous	[BMIm][PF_6]/MeOH	*L*-**2**	528	4.5	99.3	482	0.04	1
3 [d]	IL-homogeneous	[BMIm][BF_4]/MeOH	*L*-**2**	1068	4.9	97.2	335	0.02	2
4 [d]	IL-homogeneous	[BMIm][BF_4]/MeOH	*L*-**3**	1068	4.9	99.5	310	0.04	2
5 [e]	IL-homogeneous	[Bmim][NTf_2]/MeOH	*L*-**4**	769	50	98	375	0.27	3
6 [e]	IL-homogeneous	[Bmim][NTf_2]/MeOH	*L*-**5**	769	50	97			3
7 [e]	IL-homogeneous	[Bmim][NTf_2]/MeOH	BINAP	769	50	98	228	4.63	3
8 [f]	IL-homogeneous	[N_{6222}][NTf_2]/MeOH	BINAP		1335 [g]	98.3			4
9 [h]	IL-homogeneous	[BMIm][BF_4]/$scCO_2$	BINAP	209	100	97			5
10 [i]	IL-biphasic	[BMIm][BF_4]	*L*-**6**	31	66.7	86	2000		6
11 [i]	IL-biphasic	[BPy][NTf_2]	*L*-**7**	20	66.7	83			6
12 [j]	IL-biphasic	[BMIm][PF_6]/*i*-PrOH	BINAP	3469	21	97	14	0	7
13 [k]	SILP-catalysis	SiO_2-[EMIM]NTf_2/ MeOH	*L*-**8**			75-80	2500		8
14 [l]	aqueous biphasic	H_2O	*L*-**6**	none	66.7	99	8000		9
15 [m]	aqueous biphasic	H_2O	*L*-**9**	none	62.5	94	2970		10
16 [n]	aqueous biphasic	H_2O	*L*-**10**	none	50	94	5000		11
17 [o]	thermoregulated	EtOH/1,4-dioxane	*L*-**11**	none	10	97.8	383		12
18	HCBS system	MeOH	**3a**	none	333	99	12000	0.3-0.4	**Our work**

[a] Molar ratio of carrier IL to substrate. [b] Calculated based on the total reaction time. [c] *V*(IL/Co-solvent) = 0.5/0.5 mL/mL, *n*(S)/*n*(Ru) = 100/1, *n*(L)/*n*(Ru) = 1.1/1, *P*(H_2) = 10.34 MPa, *t* = 22 h, *T* = R.T., MAA as the substrate. [d] *V*(IL/Co-solvent) = 0.5/0.5 mL/mL, *n*(S)/*n*(Ru) = 100/1, *n*(L)/*n*(Ru) = 1.1/1, *P*(H_2) = 9.65 MPa, *t* = 20 h, *T* = R.T., ethyl benzoylacetate as the substrate. [e] *m*(IL) = 1 g, *V*(MeOH) = 1 mL, *n*(S)/*n*(Ru) = 100/1, *n*(L)/*n*(Ru) = 1/1, *P*(H_2) = 4 MPa, *t* = 20 h, *T* = 60˚C, MAA as the substrate. [f] *V*(IL/Co-solvent) = 8.5/8.5 mL/mL, *n*(S)/*n*(Ru) = 1580/1, *n*(L)/*n*(Ru) = 1/1, *P*(H_2) = 5 MPa, *T* = 60˚C, 1 wt.% N_{6222} Br, MAA as the substrate. [g] TOF value at 90% conversion. [h] *V*(IL) = 0.5 mL, *n*(S)/*n*(Ru) = 200/1, *n*(L)/*n*(Ru) = 1.5/1, *P*(H_2) = 2.74 MPa, *P*(CO_2) = 8.41 MPa, *t* = 1 h, *T* = 75˚C, MAA as the substrate. [i] *V*(IL) = 1 mL, *n*(S)/*n*(Ru) = 1000/1, *P*(H_2) = 4 MPa, *t* = 15 h, *T* = 50˚C, ethyl acetoacetate (EAA) as the substrate. [j] *V*(IL) = 2 mL, *V*(*i*-PrOH) = 2 mL, *n*(S)/*n*(Ru) = 140/1, *P*(H_2) = 4 MPa, *t* = 20 min, *T* = 60˚C, MAA as the substrate. [k] A continuous gas-phase reaction: *P*(H_2) = 1 MPa, *t* = 70 h, *T* = 105 °C, MAA as the substrate. [l] *V*(H_2O) = 1 mL, *n*(S)/*n*(Ru) = 1000/1, *n*(L)/*n*(Ru) =1/1, *P*(H_2) = 40 bar, *t* = 15 h, *T* = 50˚C, EAA as the substrate. [m] *V*(H_2O) = 1 mL, *n*(S)/*n*(Ru) = 1000/1, *n*(L)/*n*(Ru) = 1/1, *P*(H_2) = 4 MPa, *t* = 16 h, *T* = 50˚C, EAA as the substrate. [n] *V*(H_2O) = 2 mL, *n*(S)/*n*(Ru) = 1000/1, *n*(NaI)/*n*(Ru) = 100/1, *P*(H_2) = 4 MPa, *t* = 20 h, *T* = 60˚C, MAA as the substrate. [o] n(S)/(Ru) = 100/1, n(L)/(Ru) = 1.1/1, *P*(H_2) = 4 MPa, *t* =10 h, *T* = 60 °C, MAA as the substrate.

6. GC charts of the products

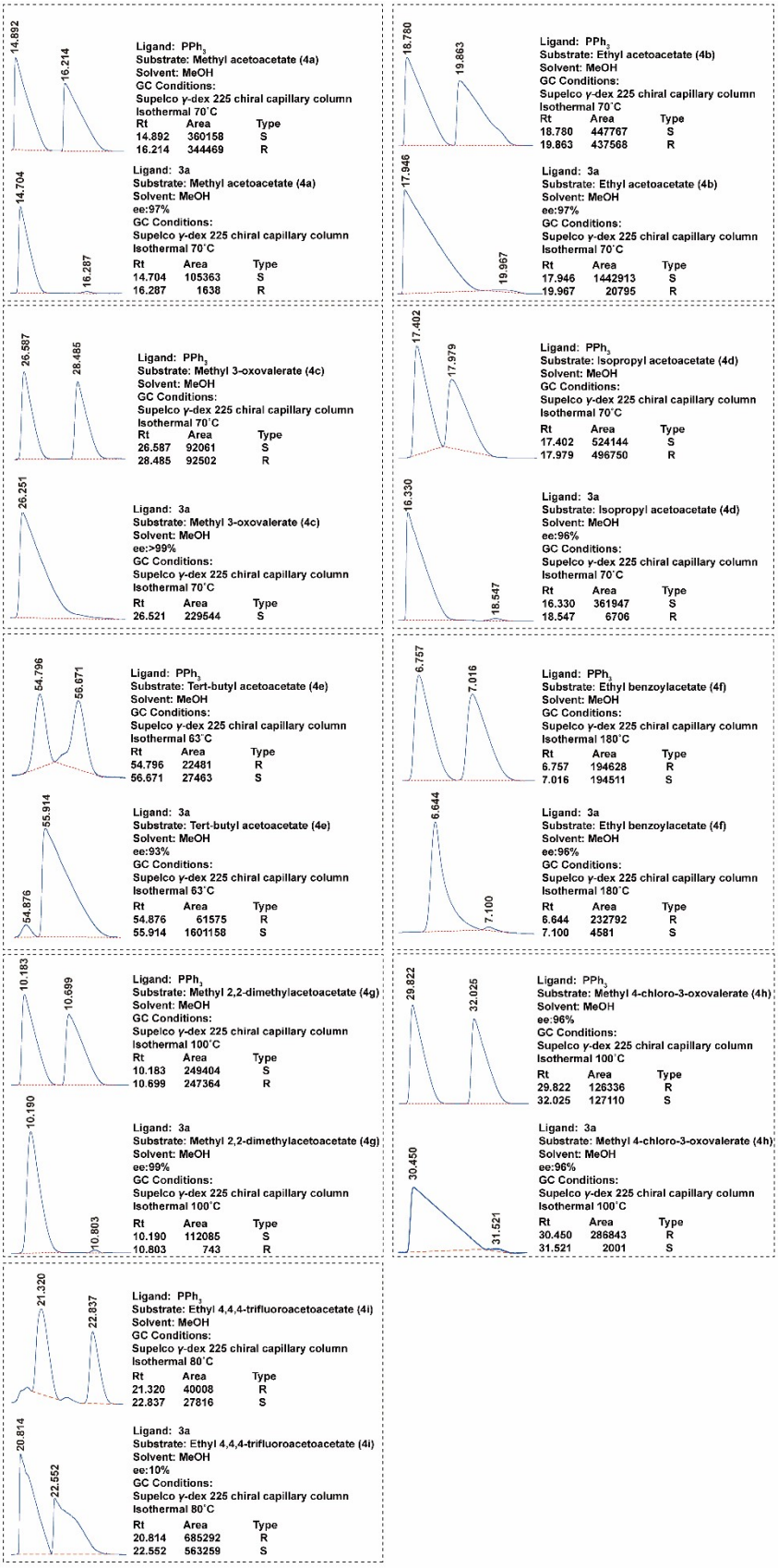

Fig. S4 GC charts of the products

7. Characterization of the products

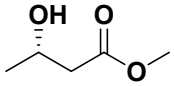

methyl (*S*)-3-hydroxybutyrate (5a) ^{1}H NMR (500 MHz, $CDCl_3$): δ = 4.233–4.176 (m, 1H), 3.717 (s, 3H), 2.935 (br, 1H), 2.524–2.408 (m, 2H), 1.235(d, 3H, *J* = 6.0 Hz).

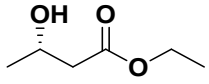

ethyl (*S*)-3-hydroxybutyrate (5b) ^{1}H NMR (500 MHz, $CDCl_3$): δ = 4.228–4.150 (m, 3H), 3.020 (br, 1H), 2.509–2.392 (m, 2H), 1.278 (t, 3H, *J* = 7 Hz), 1.231 (d, 3H, *J* = 6 Hz).

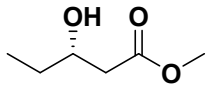

methyl (*S*)-3-hydroxyvalerate (5c) ^{1}H NMR (500 MHz, $CDCl_3$): δ = 3.970–3.912 (m, 1H), 3.716 (s, 3H), 2.865 (d, 1H, *J* = 4 Hz), 2.544–2.390 (m, 2H), 1.639–1.454 (m, 2H), 0.966 (t, 3H, *J* = 7.5 Hz).

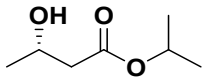

isopropyl (*S*)-3-hydroxybutyrate (5d) ^{1}H NMR (500 MHz, $CDCl_3$): δ = 5.043 (m, 1H), 4.216–4.153 (m, 1H), 3.394 (br, 1H), 2.474–2.379 (m, 2H), 1.254–1.214 (m, 9H).

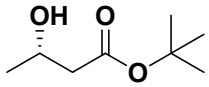

tert-butyl (*S*)-3-hydroxybutyrate (5e) ^{1}H NMR (500 MHz, $CDCl_3$): δ = 4.178–4.116 (m, 1H), 3.171 (br, 1H), 2.435–2.307 (m, 2H), 1.467 (s, 9H), 1.207 (d, 3H, *J* = 6.5Hz).

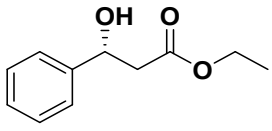

ethyl (*R*)-3-hydroxy-3-phenylpropanoate (5f) ^{1}H NMR (500 MHz, $CDCl_3$): *δ* = 7.393–7.339 (m, 4H), 7.303–7.268 (m, 1H), 5.138 (m, 1H), 4.190 (q, 2H, *J* = 7 Hz), 3.251 (br, 1H), 2.787–2.689 (m, 2H), 1.265 (t, 3H, *J* = 7 Hz).

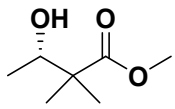

methyl (*S*)-2,2-dimethyl-3-hydroxybutyrate (5g) ^{1}H NMR (500 MHz, $CDCl_3$): *δ* = 3.867 (q, 1H, *J* = 6.5 Hz), 3.709 (s, 3H), 2.629 (br, 1H), 1.184–1.138 (m, 9H).

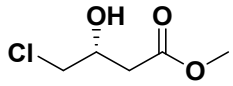

methyl (*R*)-4-chloro-3-hydroxybutyrate (5h) ^{1}H NMR (500 MHz, $CDCl_3$): δ = 4.286–4.252 (m, 1H), 3.732 (s, 1H), 3.644–3.582 (m, 2H), 3.241 (br, 1H), 2.697–2.598 (m, 2H).

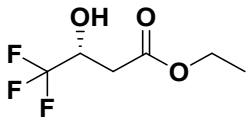

ethyl (*R*)-4,4,4-trifluoro-3-hydroxybutyrate (5i) ^{1}H NMR (500 MHz, $CDCl_3$): δ = 4.486–4.420 (m, 1H), 4.210 (q, 2H, *J* = 7 Hz), 4.14 (br, 1H), 2.738–2.642 (m, 2H), 1.288 (t, 3H, *J* = 7 Hz).

8. NMR spectra of the CPF-PILs

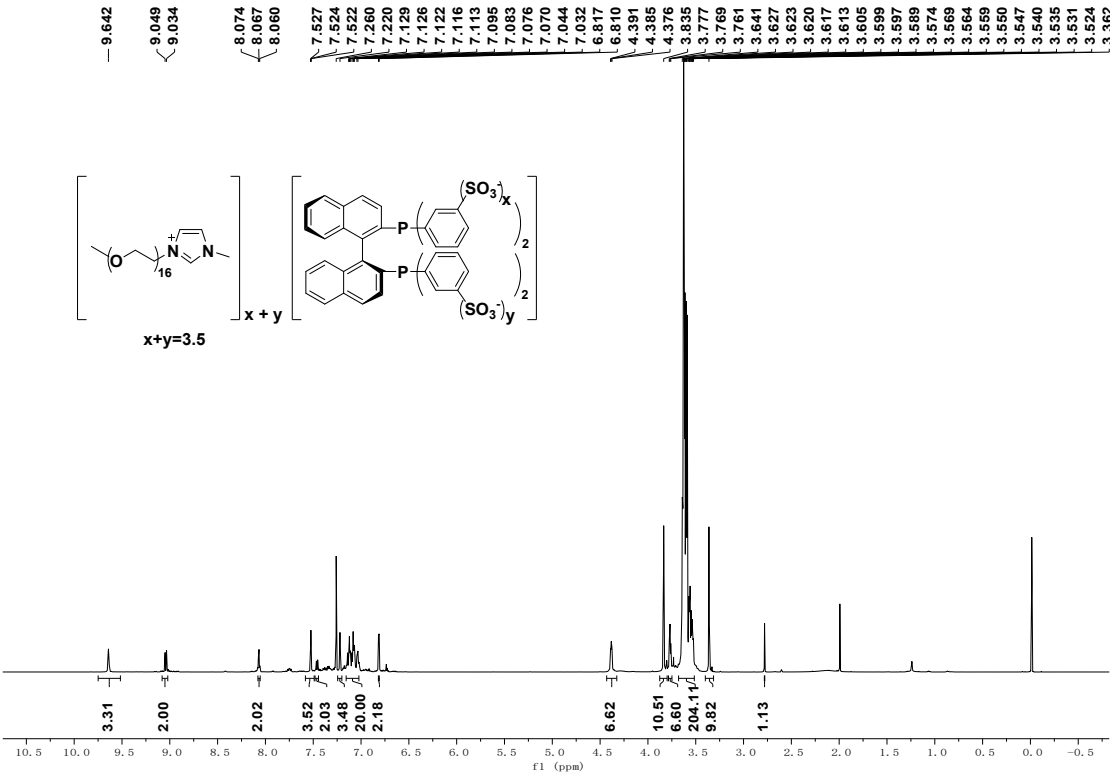

Fig. S5 ^{1}H NMR (500 MHz) spectra of the **3a** in $CDCl_3$

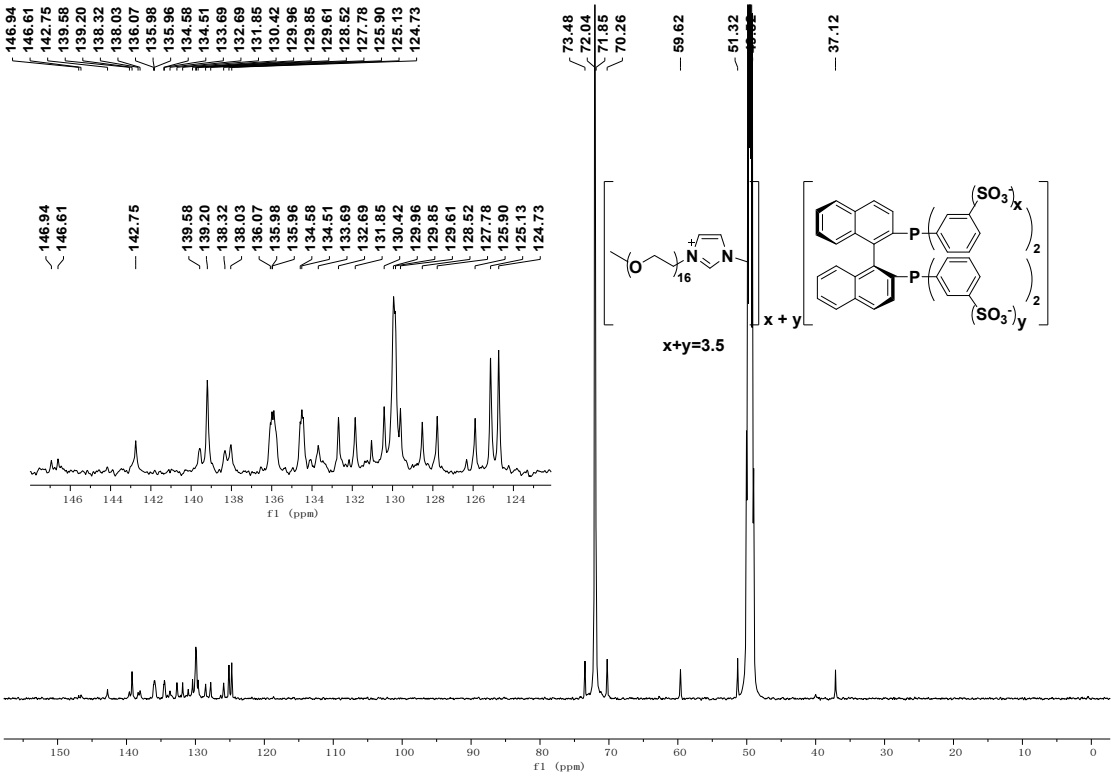

Fig. S6 ^{13}C NMR (126 MHz) spectra of the **3a** in CD_3OD

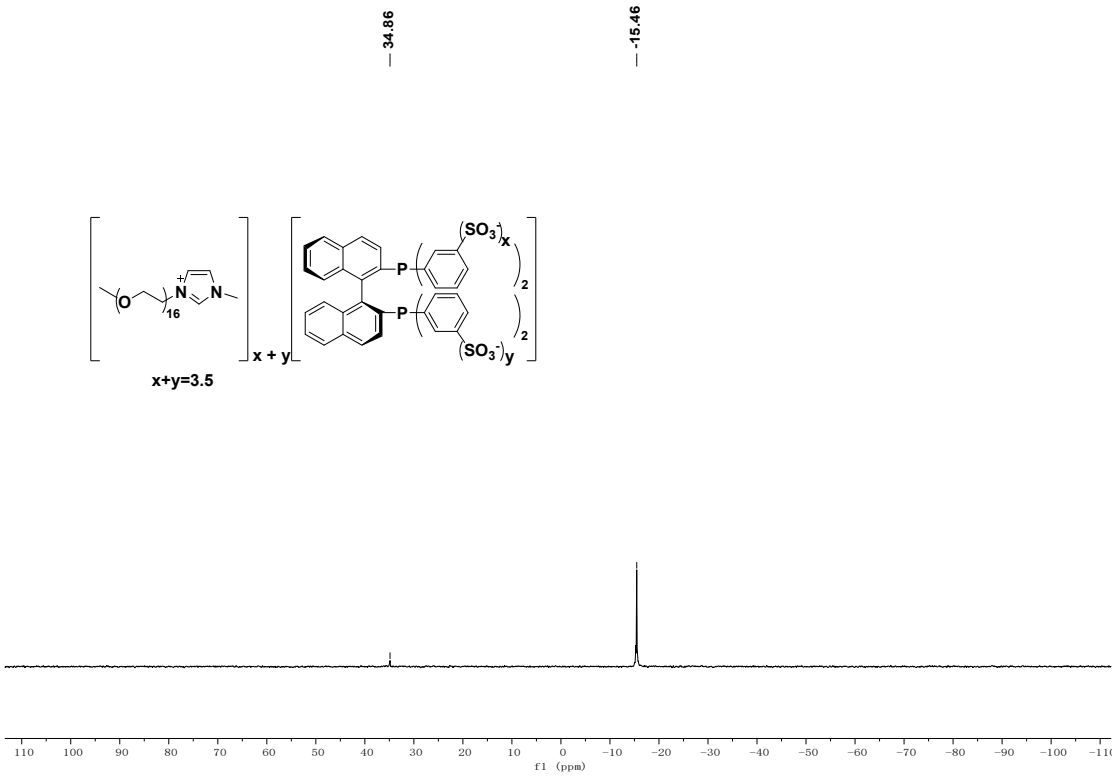

Fig. S7 ^{31}P NMR (202 MHz) spectra of the **3a** in D_2O

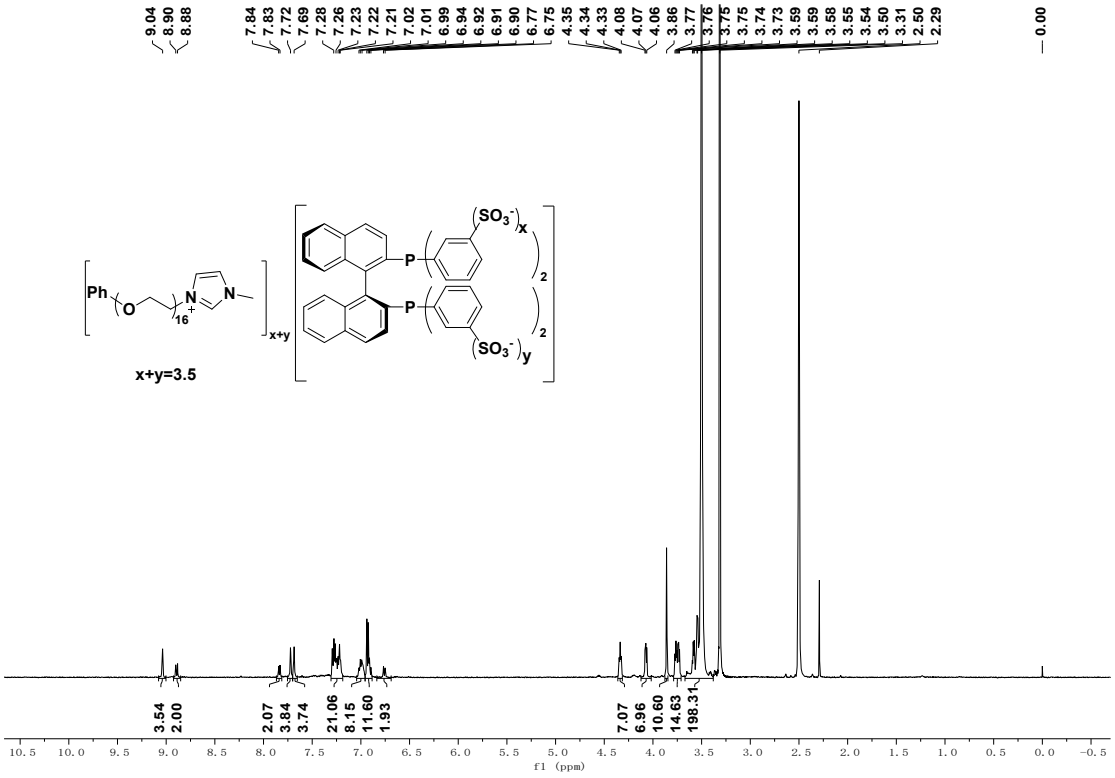

Fig. S8 ^{1}H NMR (500 MHz) spectra of the **3b** in DMSO-d_6

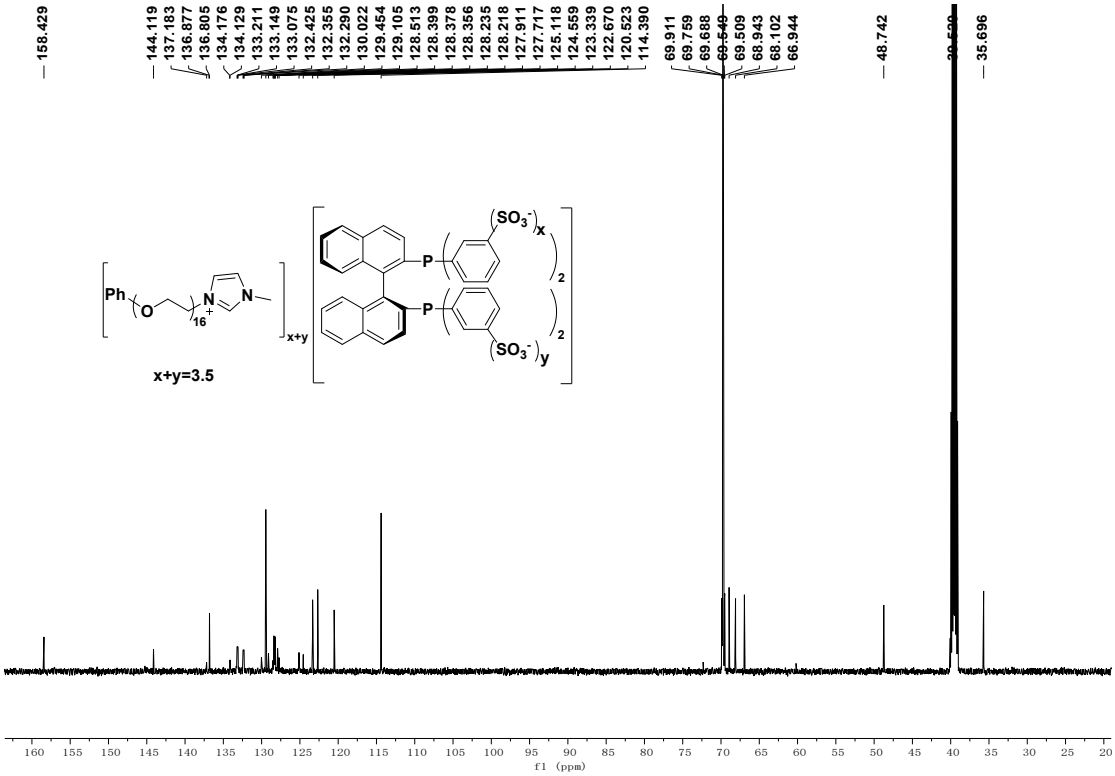

Fig. S9 ^{13}C NMR (151 MHz) spectra of the **3b** in DMSO-d_6

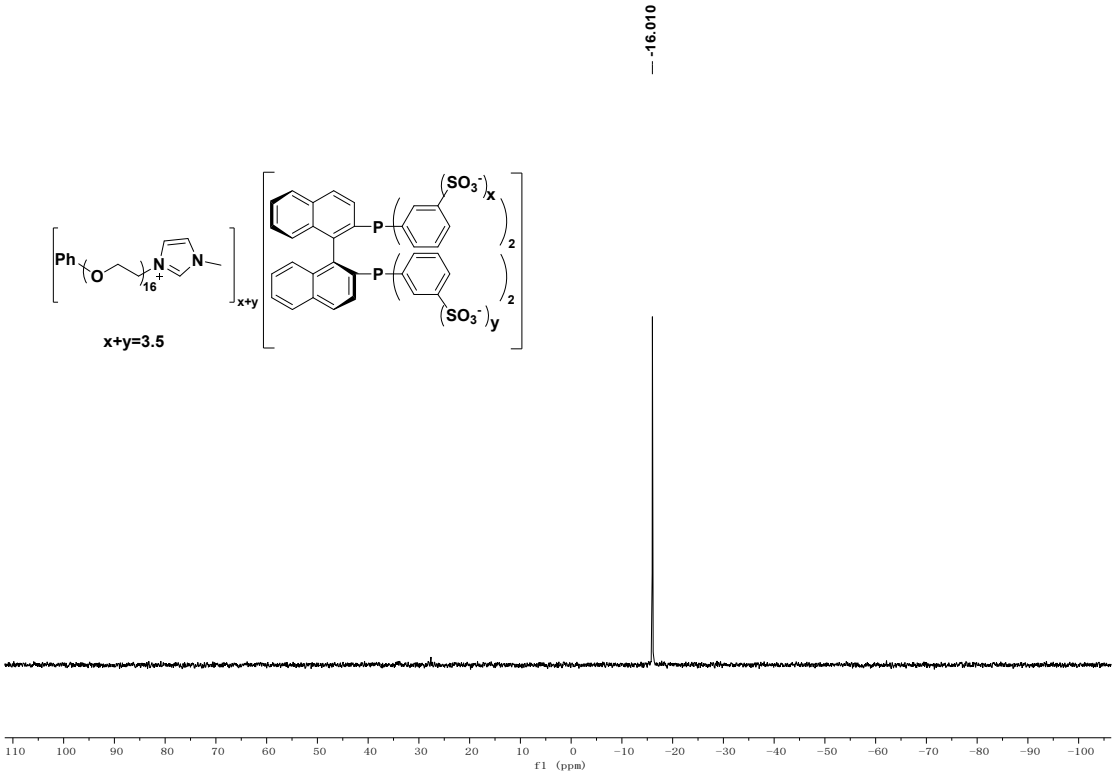

Fig. S10 ^{31}P NMR (202 MHz) spectra of the **3b** in $CDCl_3$

9. NMR spectra of the products

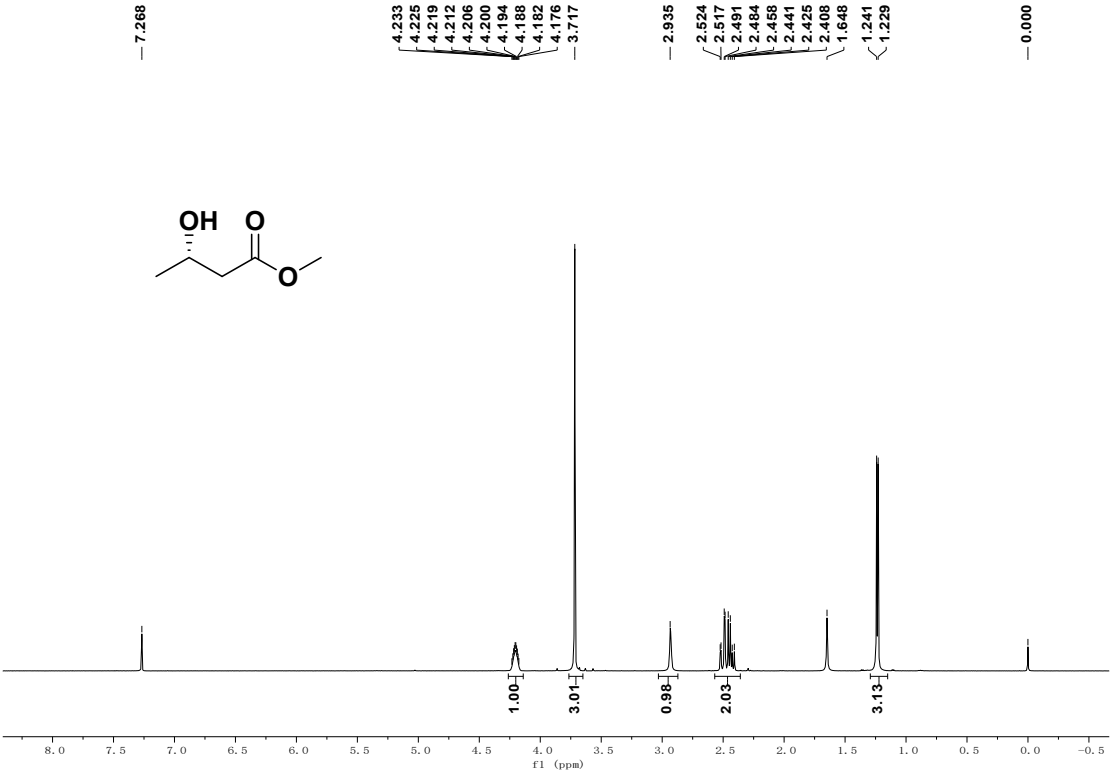

Fig. S11 ^{1}H NMR (500 MHz) spectra of the methyl (*S*)-3-hydroxybutyrate (**5a**) in $CDCl_3$

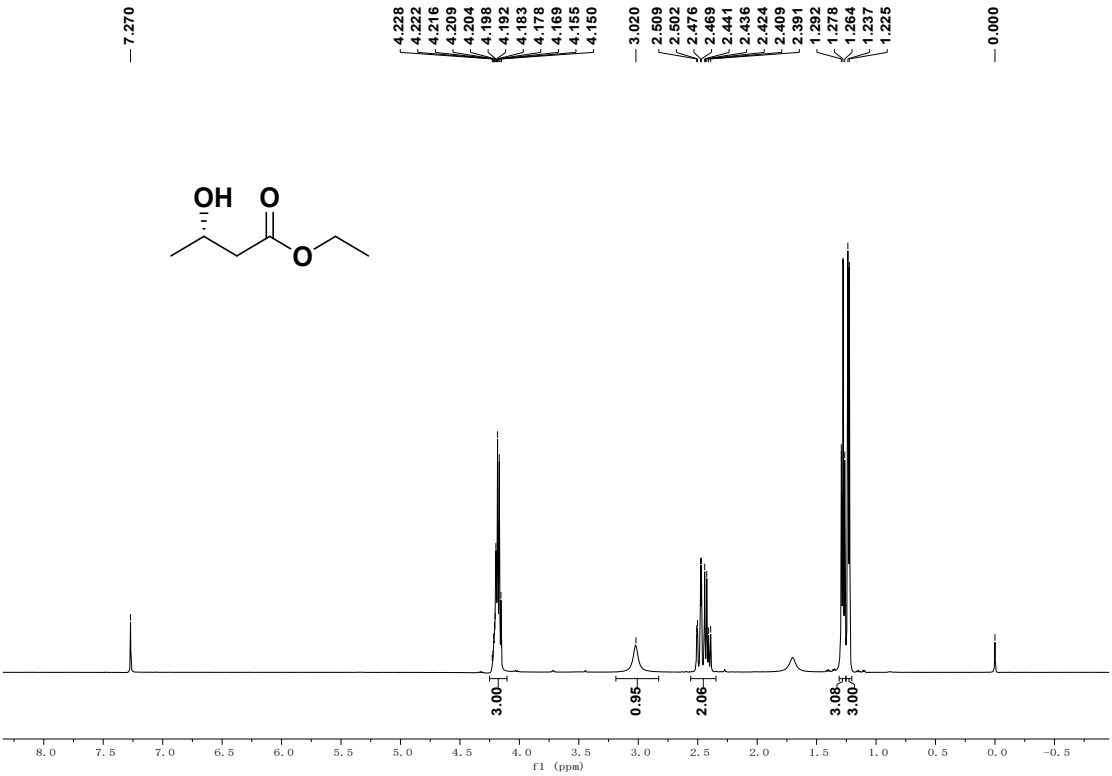

Fig. S12 ^{1}H NMR (500 MHz) spectra of the ethyl (*S*)-3-hydroxybutyrate (**5b**) in $CDCl_3$

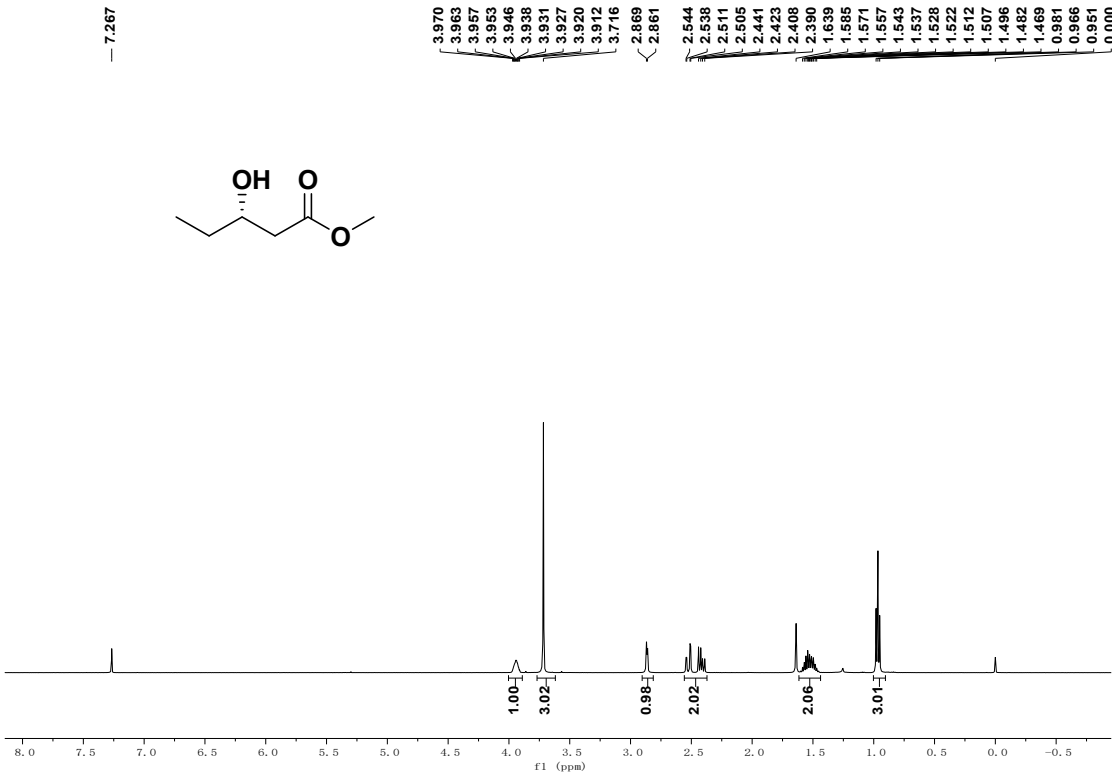

Fig. S13 ^{1}H NMR (500 MHz) spectra of the methyl (*S*)-3-hydroxyvalerate (**5c**) in $CDCl_3$

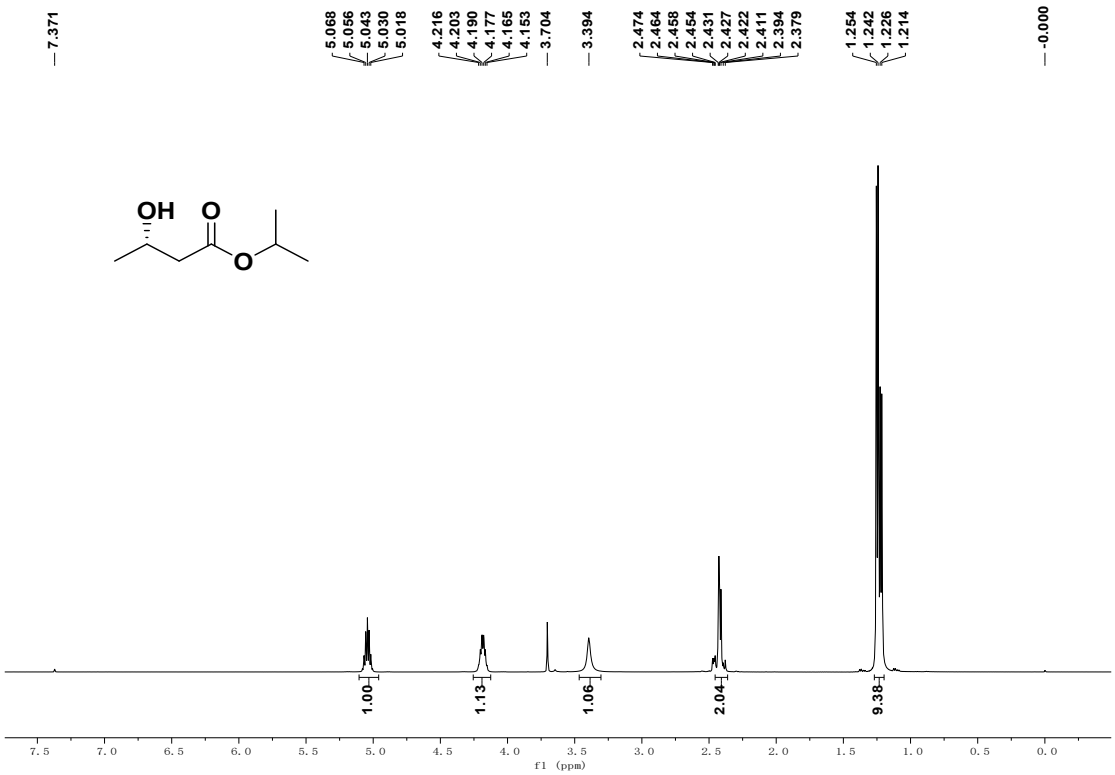

Fig. S14 ^{1}H NMR (500 MHz) spectra of the isopropyl (*S*)-3-hydroxybutyrate (**5d**) in $CDCl_3$

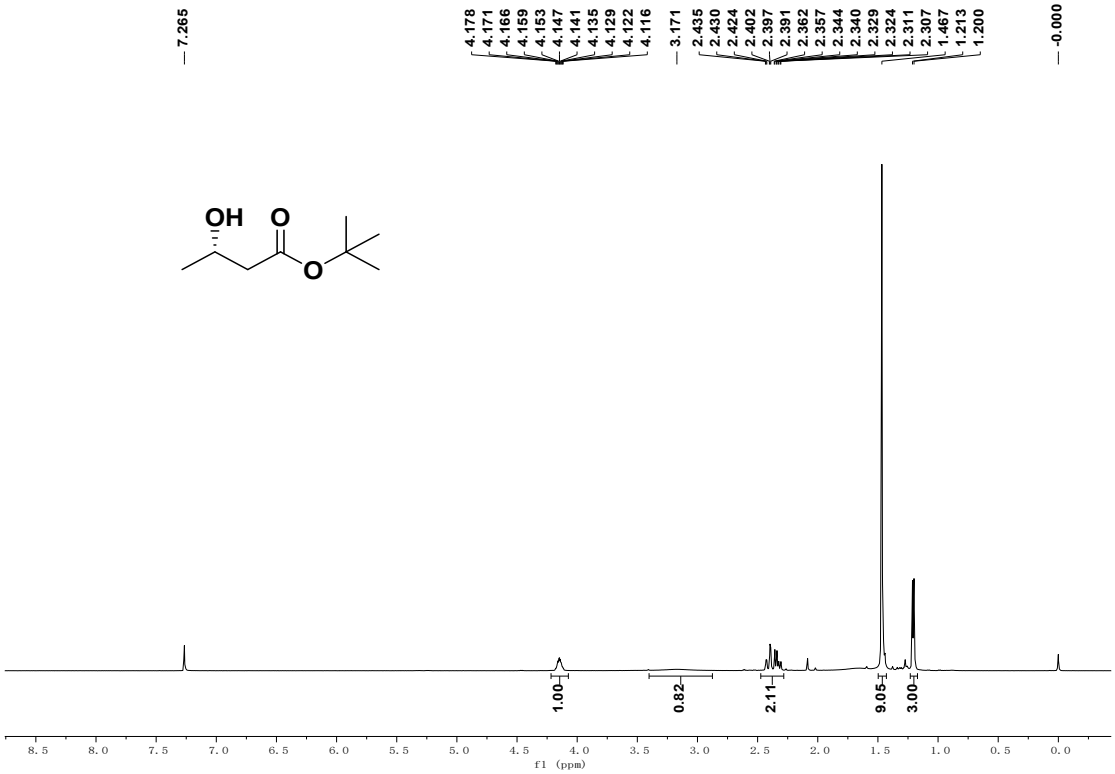

Fig. S15 ^{1}H NMR (500 MHz) spectra of the tert-butyl (*S*)-3-hydroxybutyrate (**5e**) in $CDCl_3$

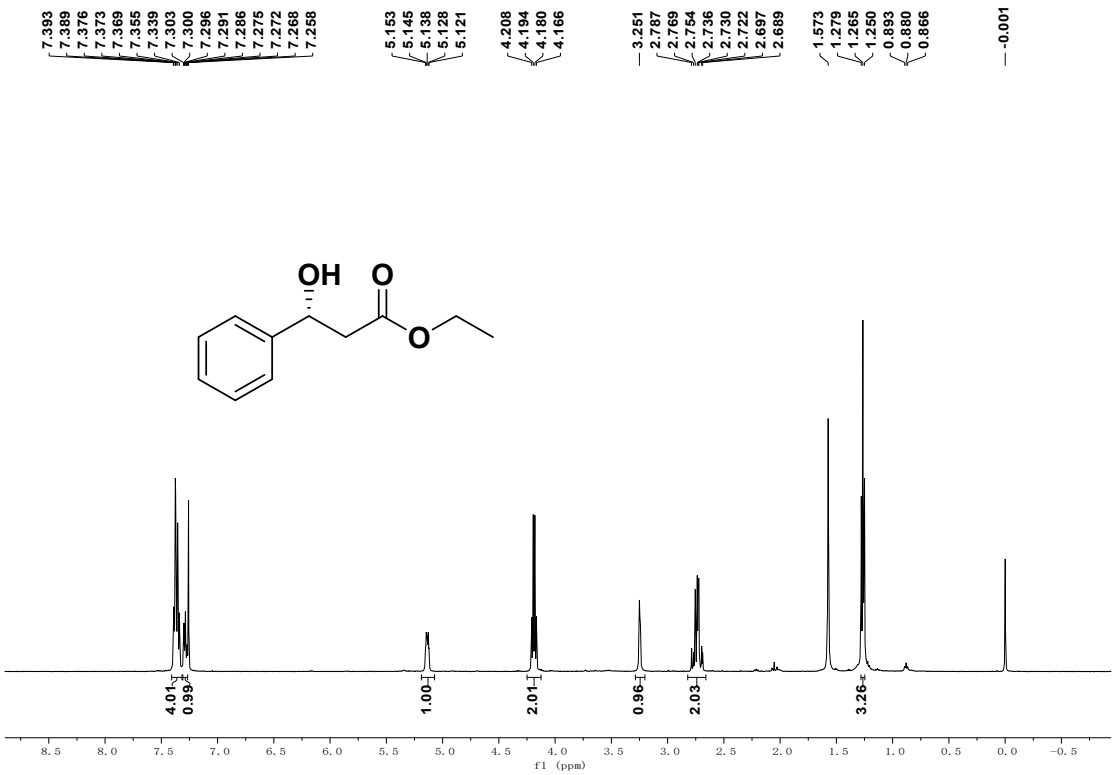

Fig. S16 ^{1}H NMR (500 MHz) spectra of the ethyl (*R*)-3-hydroxy-3-phenylpropanoate (**5f**) in $CDCl_3$

Fig. S17 ^{1}H NMR (500 MHz) spectra of the methyl (*S*)-2,2-dimethyl-3-hydroxybutyrate (**5g**) in $CDCl_3$

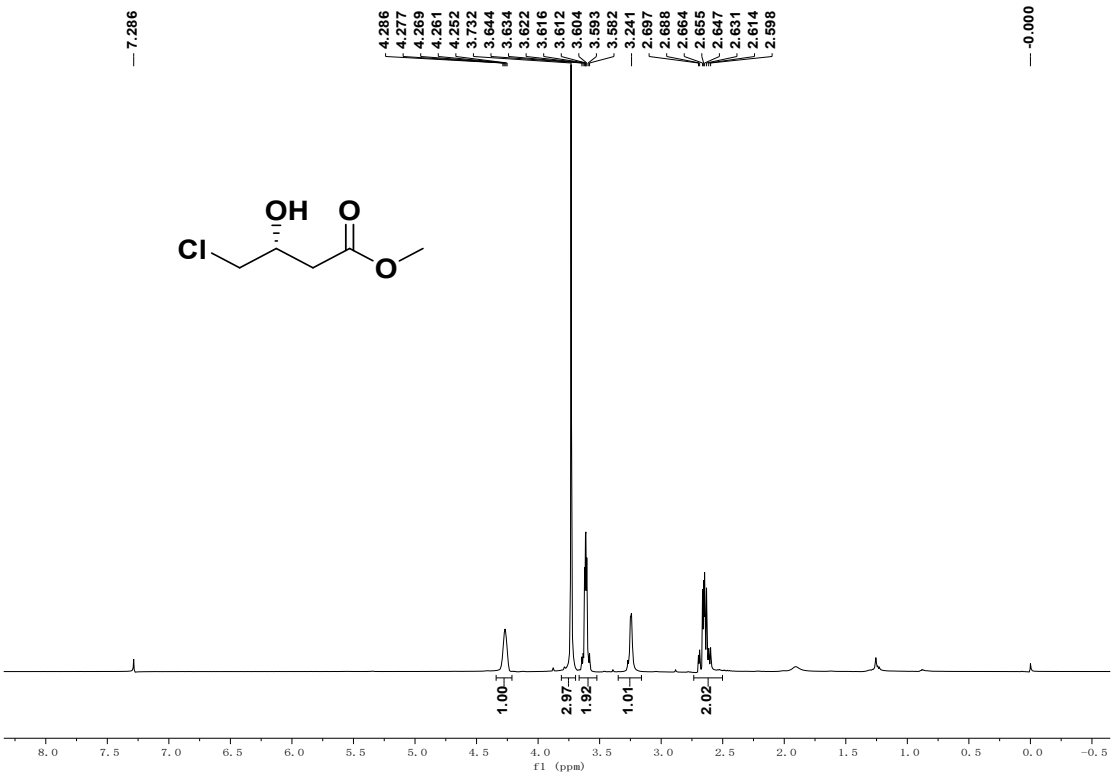

Fig. S18 ^{1}H NMR (500 MHz) spectra of the methyl (*R*)-4-chloro-3-hydroxybutyrate (**5h**) in $CDCl_3$

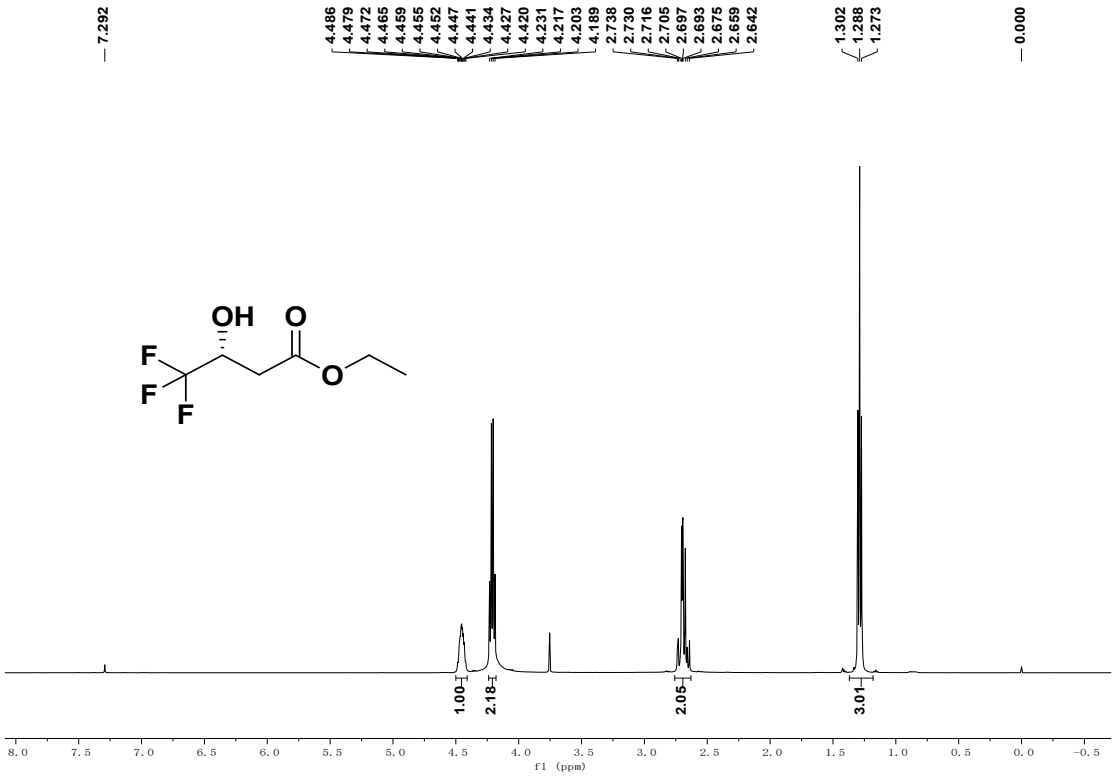

Fig. S19 ^{1}H NMR (500 MHz) spectra of the ethyl (*R*)-4,4,4-trifluoro-3-hydroxybutyrate (**5i**) in $CDCl_3$

10. HRMS spectra of the CPF-PILs

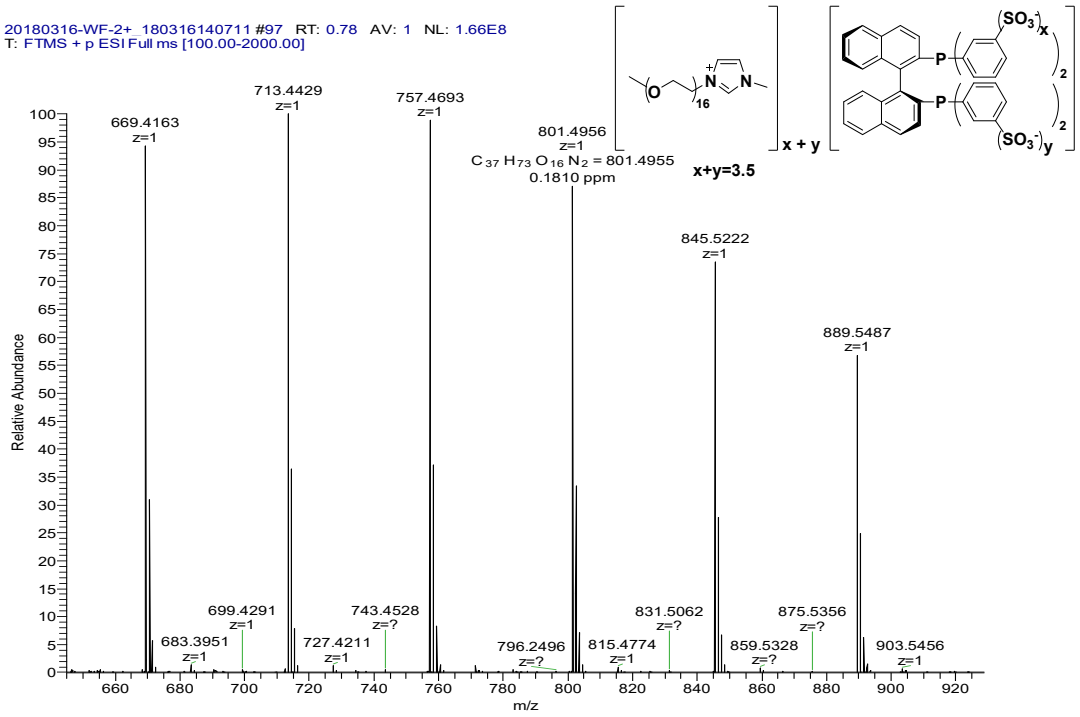

Fig. S20 Mass spectrum (ESI positive) of **3a**

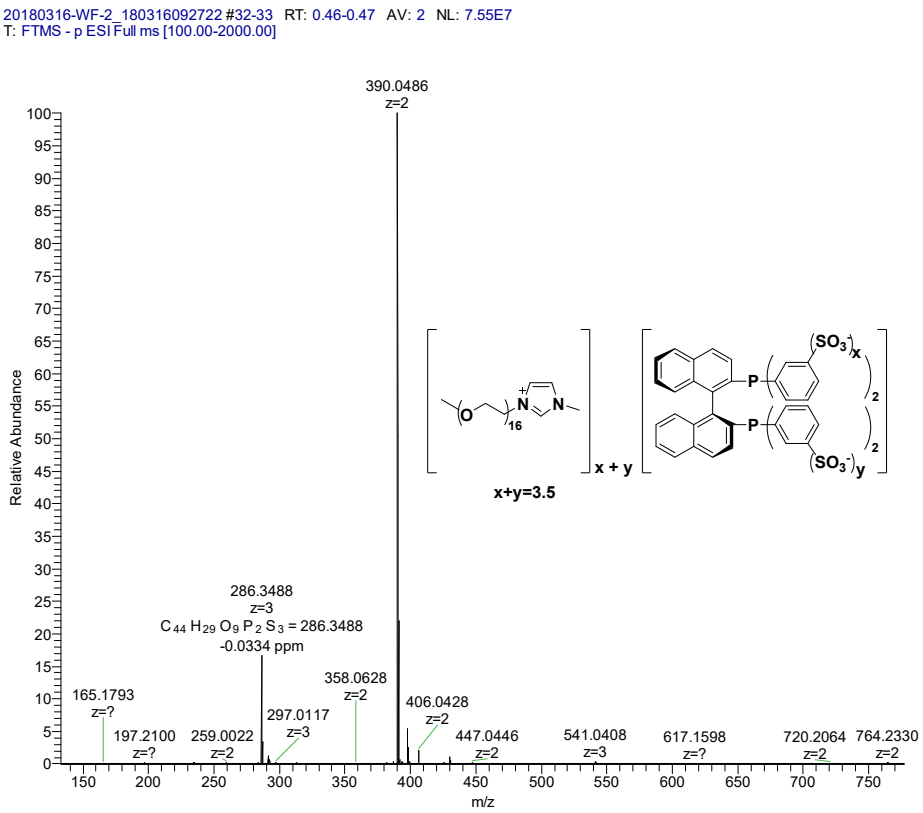

Fig. S21 Mass spectrum (ESI negative) of **3a**

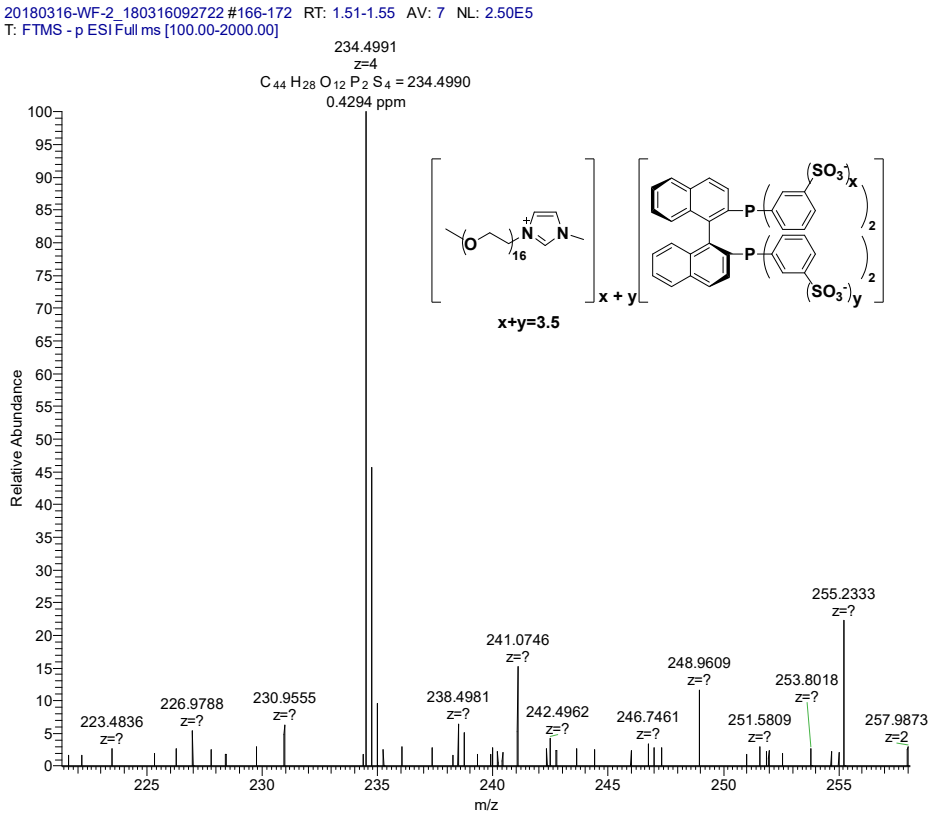

Fig. S22 Mass spectrum (ESI negative) of **3a**

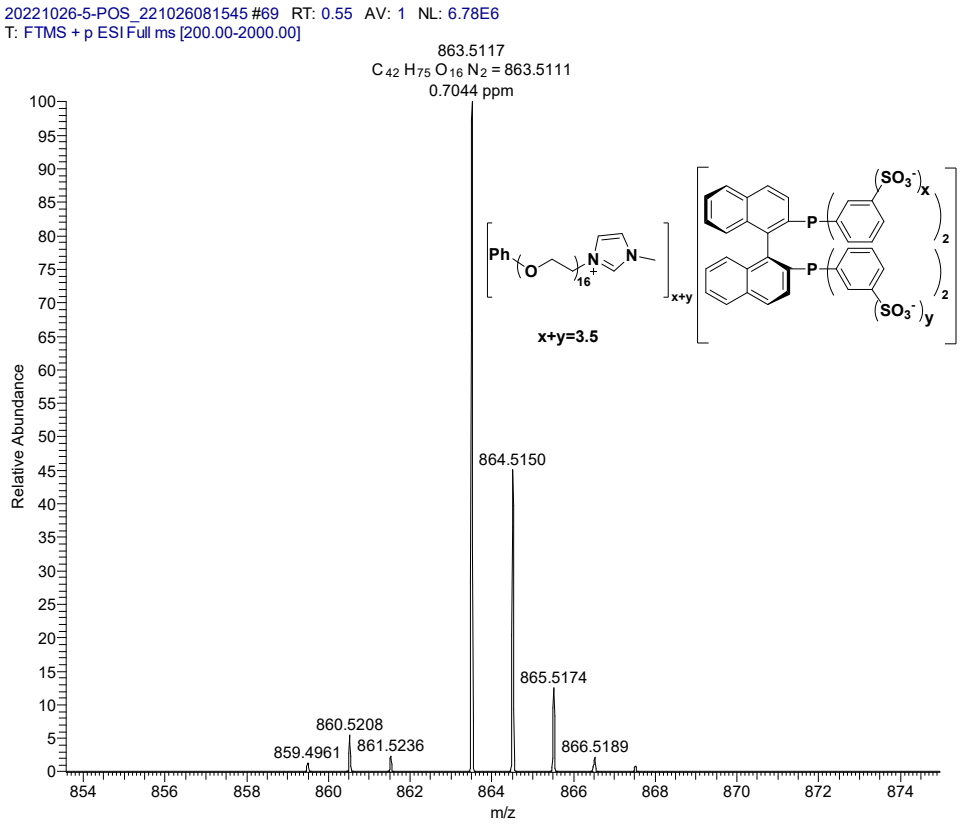

Fig. S23 Mass spectrum (ESI positive) of **3b**

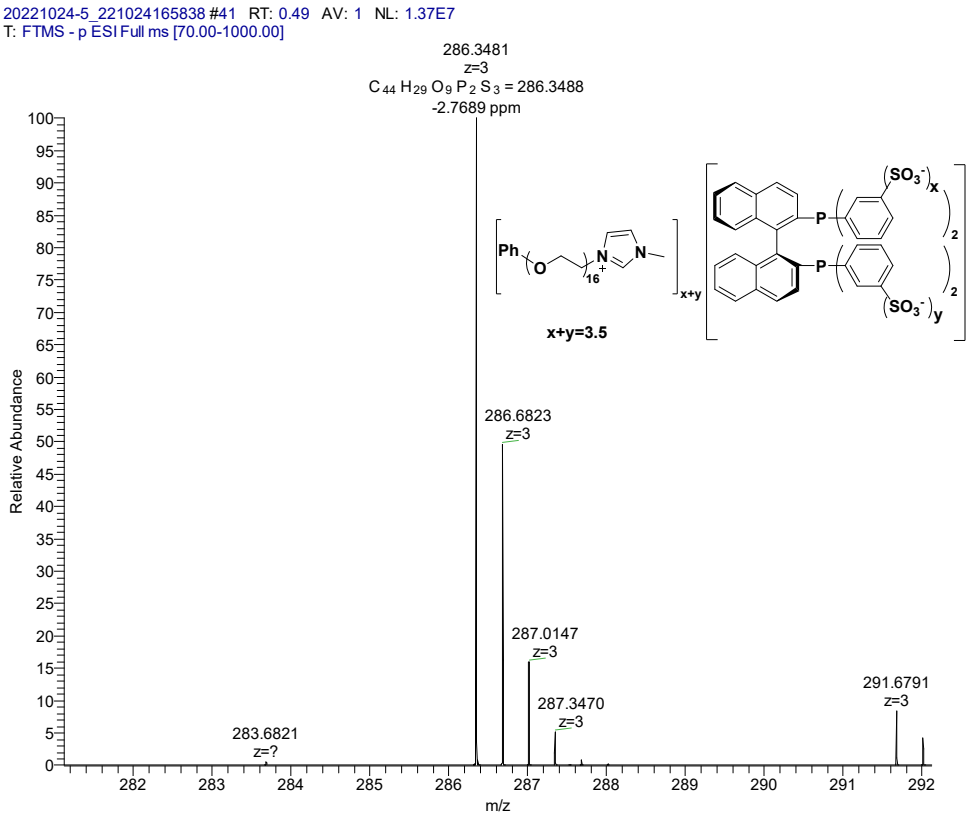

Fig. S24 Mass spectrum (ESI negative) of **3b**

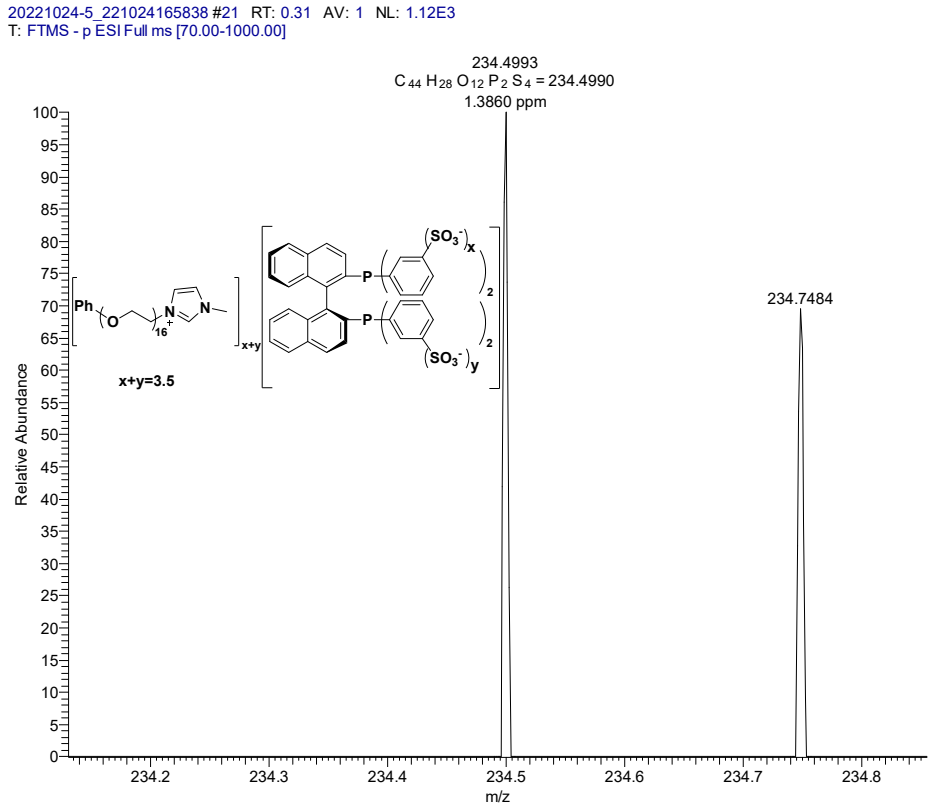

Fig. S25 Mass spectrum (ESI negative) of **3b**

11. Reference

1 H. L. Ngo, A. Hu and W. Lin, Highly enantioselective catalytic asymmetric hydrogenation of β-keto esters in room temperature ionic liquids, *Chem. Commun.*, 2003, **15**, 1912─1913.

2 A. Hu, H. L. Ngo and W. Lin, Remarkable 4,4′-substituent effects on BINAP: highly enantioselective Ru catalysts for asymmetric hydrogenation of β-aryl ketoesters and their immobilization in room-temperature ionic liquids, *Angew. Chem. Int. Ed.*, 2004, **116**, 2555─2558.

3 X. Jin, F. Kong, Z. Yang and F. Cui, Synthesis of BINAP ligands with imidazole tags for highly enantioselective Ru-catalyzed asymmetric hydrogenation of β-keto esters in ionic liquid systems, *J. Mol. Catal. A-Chem.*, 2013, **374**, 22─26.

4 T. Floris, P. Kluson, L. Bartek and H. Pelantova, Quaternary ammonium salts ionic liquids for immobilization of chiral Ru-BINAP complexes in asymmetric hydrogenation of β-ketoesters, *Appl. Catal. A,* 2009, **366**, 160─165.

5 O. V. Turova, I. V. Kuchurov, E. V. Starodubtseva, V. A. Ferapontov, N. S. Ikonnikov, S. G. Zlotin and M. G. Vinogradov, Ru-BINAP-catalyzed asymmetric hydrogenation of keto esters in high pressure carbon dioxide, *Mendeleev Commun.*, 2012, **4**, 184─186.

6 M. Berthod, J. M. Joerger, G. Mignani, M. Vaultier and M. Lemaire, Enantioselective catalytic asymmetric hydrogenation of ethyl acetoacetate in room temperature ionic liquids, *Tetrahedron: Asymmetry*, 2004, **15**, 2219–2221.

7 A. Wolfson, I. F. J. Vankelecom and P. A. Jacobs, The role of additional solvents in transition metal complex catalyzed asymmetric reductions in ionic liquid containing systems, *J. organomet. chem.*, 2005, **690**, 3558–3566.

8 E. Öchsnera, M. J. Schneidera, C. Meyera, M. Haumannb and P. Wasserscheid, Challenging the scope of continuous, gas-phase reactions with supported ionic liquid phase (SILP) catalysts—Asymmetric hydrogenation of methyl acetoacetate, *Appl. Catal., A*, 2011, **399**, 35–41.

9 M. Berthod, C. Saluzzo, G. Mignani and M. Lemaire, 4, 4′ and 5, 5′-DiamBINAP as a hydrosoluble chiral ligand: syntheses and use in Ru(II) asymmetric biphasic catalytic hydrogenation, *Tetrahedron: Asymmetry*, 2004, **15**, 639–645.

10 T. Lamouille, C. Saluzzo, R. T. Halle and F. L. Guyader, Hydrogenation of ethyl acetoacetate catalyzed by hydrosoluble BINAP derivatives, *Tetrahedron Lett.*, 2001, **42**, 663–664.

11 X. Jin, S. Huang, F. Wang, L. Zhu, H. Song, C. Xie, S. Yu and S. Li, Synthesis and characterization of a high-purity chiral 5,5'-disulfonato-BINAP ligand and its application in asymmetric hydrogenation of β-keto esters, *Mol. Catal.*, 2021, **507**, 111562.

12 Y.-Y. Huang, Y.-M. He, H.-F. Zhou, L. Wu, B.-L. Li and Q.-H. Fan, Thermomorphic system with non-fluorous phase-tagged Ru (BINAP) catalyst: Facile liquid/solid catalyst separation and application in asymmetric hydrogenation *J. Org. Chem.*, 2006, **71**, 2874–2877.